

## Metalorganic chemical vapor deposition of aluminum oxide on Si: Evidence of interface SiO<sub>2</sub> formation

A. Roy Chowdhuri, C. G. Takoudis, R. F. Klie, and N. D. Browning

Citation: [Applied Physics Letters](#) **80**, 4241 (2002); doi: 10.1063/1.1483903

View online: <http://dx.doi.org/10.1063/1.1483903>

View Table of Contents: <http://scitation.aip.org/content/aip/journal/apl/80/22?ver=pdfcov>

Published by the [AIP Publishing](#)

---

### Articles you may be interested in

[Energy-band parameters of atomic layer deposited Al<sub>2</sub>O<sub>3</sub> and HfO<sub>2</sub> on In<sub>x</sub>Ga<sub>1-x</sub>As](#)  
Appl. Phys. Lett. **94**, 052106 (2009); 10.1063/1.3078399

[Mechanisms of SiO<sub>2</sub> film deposition from tetramethylcyclotetrasiloxane, dimethyldimethoxysilane, and trimethylsilane plasmas](#)  
J. Vac. Sci. Technol. A **22**, 201 (2004); 10.1116/1.1635392

[Thermal annealing effects on the structural and electrical properties of HfO<sub>2</sub> / Al<sub>2</sub>O<sub>3</sub> gate dielectric stacks grown by atomic layer deposition on Si substrates](#)  
J. Appl. Phys. **94**, 2563 (2003); 10.1063/1.1590414

[Analysis of ultrathin SiO<sub>2</sub> interface layers in chemical vapor deposition of Al<sub>2</sub>O<sub>3</sub> on Si by in situ scanning transmission electron microscopy](#)  
Appl. Phys. Lett. **83**, 1187 (2003); 10.1063/1.1597415

[Interfacial layer formation during high-temperature annealing of ZrO<sub>2</sub> thin films on Si](#)  
Appl. Phys. Lett. **81**, 3431 (2002); 10.1063/1.1517407

---



## Re-register for Table of Content Alerts

Create a profile.



Sign up today!



# Metalorganic chemical vapor deposition of aluminum oxide on Si: Evidence of interface SiO<sub>2</sub> formation

A. Roy Chowdhuri and C. G. Takoudis<sup>a)</sup>

Department of Chemical Engineering (M/C 110), University of Illinois at Chicago, 810 S. Clinton Street, Chicago, Illinois 60607-7000

R. F. Klie and N. D. Browning

Department of Physics (M/C 273), University of Illinois at Chicago, 845 West Taylor Street, Chicago, Illinois 60607-7059

(Received 7 February 2002; accepted for publication 10 April 2002)

Thin films of aluminum oxide were deposited on H-passivated Si(100) substrate using trimethylaluminum and oxygen at 0.5 Torr and 300 °C. Fourier transform infrared (FTIR) and x-ray photoelectron spectroscopic analyses of these films showed no aluminum silicate phase at the film–substrate interface. The O/Al ratio in the deposited film was found to be higher than that in stoichiometric Al<sub>2</sub>O<sub>3</sub>. On annealing the *as-deposited* samples in Ar at 900 °C, an absorption peak due to the transverse optical phonon for the Si—O—Si stretching mode appeared in the FTIR spectra. A combination of Z-contrast imaging and electron energy-loss spectroscopy in the scanning transmission electron microscope confirmed that the annealed samples developed a layer of silicon dioxide at the aluminum oxide–Si interface. Our results suggest that excess oxygen present in the deposited film reacts with the underlying Si substrate and forms silicon oxide. © 2002 American Institute of Physics. [DOI: 10.1063/1.1483903]

Aluminum oxide has emerged as one of the promising substitutes for the SiO<sub>2</sub> dielectric layer in complementary metal–oxide–semiconductor device fabrication.<sup>1</sup> It provides many advantages over other potential candidates in several aspects. With a dielectric constant ( $\epsilon_{\text{Al}_2\text{O}_3} \sim 9$ ) more than twice that of SiO<sub>2</sub> ( $\epsilon_{\text{SiO}_2} \sim 3.9$ ), Al<sub>2</sub>O<sub>3</sub> has a band gap of  $\sim 9$  eV, a 2.8 eV conduction band offset to Si, and it is robust enough to withstand high-temperature wafer processing steps. Under normal processing conditions, Al<sub>2</sub>O<sub>3</sub> is amorphous, although  $\gamma$ -alumina (cubic) may form at high temperature ( $>750$  °C).<sup>2,3</sup> Both amorphous Al<sub>2</sub>O<sub>3</sub> ( $<350$  °C) and cubic alumina ( $>750$  °C) form a thermodynamically stable interface<sup>2</sup> on Si. One study,<sup>4</sup> involving atomic layer controlled deposition using trimethylaluminum (TMA) and H<sub>2</sub>O, pointed out that Al<sub>2</sub>O<sub>3</sub> was formed without *any* aluminum silicate phase at the interface when the Si substrate was treated with HF prior to the deposition. However, another study<sup>5</sup> reported aluminum silicate phase formation at the oxide substrate interface when triethylaluminum tri-sec-butoxide and O<sub>2</sub> (at  $\sim 400$  °C) was used.

TMA has been used in thermal as well as plasma enhanced chemical vapor deposition of alumina films,<sup>4,6</sup> at temperatures lower than 400 °C. The widespread use of TMA is primarily due to its high vapor pressure at room temperature and high pyrolytic decomposition temperature ( $>350$  °C), which allows its use over a wide temperature range. In most studies involving TMA, H<sub>2</sub>O was used as the oxygen source. Recently, reaction of TMA with oxygen has been studied using a matrix isolation technique.<sup>7</sup>

In this work, we explore the use of TMA and oxygen for low-temperature metalorganic chemical vapor deposition of

aluminum oxide films on Si and characterize the deposited films and their interfaces with the substrate using a combination of Fourier-transform infrared (FTIR) spectroscopy and x-ray photoelectron spectroscopy (XPS). While the traditional method of investigating interfaces, transmission electron microscopy (TEM), provides a high degree of spatial resolution, it is not sensitive to small local changes in composition and electronic structure. However a combination of Z-contrast imaging and electron energy-loss spectroscopy (EELS), that has been used here, can provide an accurate description of the structure and chemistry of the interface with high spatial resolution.

Ultrathin aluminum oxide films were deposited using TMA (Akzo Nobel) and oxygen in a custom-made low pressure chemical vapor deposition chamber.<sup>8</sup> The sample was heated with a quartz halogen lamp and a proportional integral differential controller (Eurotherm Inc., Virginia) was used to maintain the substrate temperature within  $\pm 2$  °C during operation at 0.5 Torr. Bubbling Ar at 30 cm<sup>3</sup> min (at 1 atm and 25 °C) delivered the organometallic precursor into the chamber.

Double polished 4 in. *n*-Si(100) floating zone wafers, diced into 15 mm  $\times$  22 mm samples, were rinsed in deionized water (NANO pure water system, Barnstead, Dubuque, IA), followed by treatments in H<sub>2</sub>SO<sub>4</sub>:H<sub>2</sub>O<sub>2</sub> (1:2) to remove organic contamination and a 30 s dip in buffered HF (NH<sub>4</sub>F: 49% HF, 10:1) to remove the native oxide. In a typical operation, after sample loading, the chamber was purged with Ar at 0.1 Torr, while the sample temperature was ramped to the desired setpoint. This was followed by alternate exposures of TMA and O<sub>2</sub>, each for 30 s, with Ar purging in between each reactant exposure.

FTIR normal incidence transmission spectroscopy (Nicolet, Magna-IR 560) over the wavenumber range of

<sup>a)</sup>Electronic mail: takoudis@tiger.cc.uic.edu

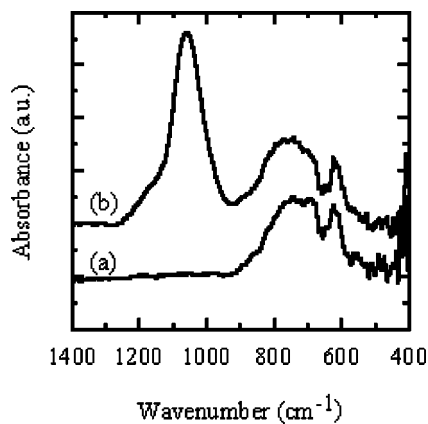


FIG. 1. FTIR spectra of 5 nm aluminum-oxide film on H-passivated Si deposited at 300 °C; *as-deposited* (a); after 25 min annealing at 900 °C in Ar (b). The TO phonon associated with the asymmetric stretch of the O in Si—O—Si bridging bond is present in the annealed sample.

4000 to 400  $\text{cm}^{-1}$  was used. The sample thickness was measured with spectroscopic ellipsometry (J. A. Woollam Co., Inc., Model M-44). XPS (Kratos, AXIS Ultra XPS) analyses of the samples were used to evaluate the bonding states and atomic composition. The scanning tunneling electron microscopy (STEM) and EELS results presented in this letter were obtained using a JEOL 2010F STEM/TEM, having a Schottky field emission gun source and being operated at 200 kV.<sup>9,10</sup> It is equipped with a standard UHR “ultrahigh resolution” objective lens pole piece, a JEOL annular dark-field detector and a postcolumn Gatan imaging filter.<sup>9,10</sup> The lens conditions in the microscope were defined for a probe size of 0.2 nm, with a convergence angle of 13 mrad and a collection angle of 52 mrad. With these settings, the probe current is sufficient (40 pA) to obtain statistically significant information and Z-contrast image is incoherent; i.e., a direct image of the interface is acquired. The experimental setup for this microscope allows us to use low-angle scattered electrons that do not contribute to the Z-contrast image for EELS.<sup>11</sup> As the two techniques do not interfere, Z-contrast images can be used to position the electron probe at the desired spot in the sample to acquire spectra.<sup>12–14</sup> The experimental conditions in the microscope mean that beam damage is always a potential issue. However, for the results obtained here, several spectra with acquisition times of  $\sim 0.5$  s are acquired consecutively in each position and compared to ensure that the beam damage is not contributing significantly to the observed spectral changes.

Figure 1(a) shows the FTIR absorbance spectra of a 5 nm aluminum oxide film deposited at 300 °C, on clean oxide-free Si(100). The broad features that appear in the range of 500 to 1000  $\text{cm}^{-1}$  are characteristic of aluminum oxide. O—Al—O bending mode appears in the range of 650 to 700  $\text{cm}^{-1}$ .<sup>6</sup> The Al—O stretching mode appears as a broad band over 750 to 850  $\text{cm}^{-1}$ .<sup>6,15</sup> The overlapping of these two modes gives rise to the wide band with two distinct peaks<sup>16</sup> at  $\sim 690$  and 745  $\text{cm}^{-1}$ . The absorption band at 610  $\text{cm}^{-1}$  is due to Al—O stretching in condensed  $\text{AlO}_6$  octahedral.<sup>17–19</sup> No spectral feature is present at 1345  $\text{cm}^{-1}$  indicating the absence of any Al=O in the film.<sup>15</sup> The absence of any Si—O in the film is suggested by the absence of any feature near 1060  $\text{cm}^{-1}$  corresponding to the transverse

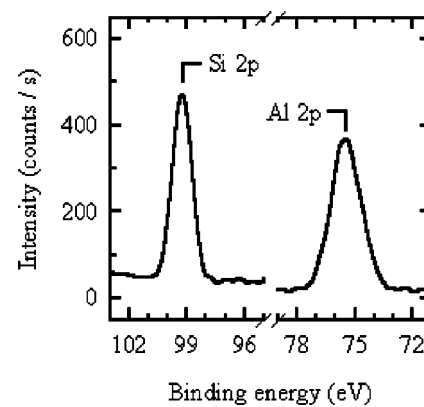


FIG. 2. XPS spectra of *as-deposited* 5 nm aluminum-oxide film on H-passivated Si deposited at 300 °C, showing the Si 2*p*, and Al 2*p*.

optical (TO) phonon associated with the asymmetric stretch of the O in Si—O—Si bridging bond. Also worth mentioning is the absence of any feature due to Si—O—Al mixed vibrations, which appear<sup>18</sup> above 1000  $\text{cm}^{-1}$ .

XPS analysis of a 5 nm aluminum oxide film deposited at 300 °C, on clean oxide-free Si (100) is presented in Fig. 2. The Si 2*p* signal<sup>5,20</sup> at 99.3 eV is due to Si<sup>0</sup>, however, no signal from Si<sup>*n*>0</sup> states is present. A previous study reporting aluminum silicate phase formation near the interface during chemical vapor deposition of  $\text{Al}_2\text{O}_3$ , assigned a peak near 102 eV to Al in Al—O—Si bonds.<sup>5</sup> Beside such bonds, presence of Si<sup>2+</sup> in the Si 2*p* spectra of a 3.5 nm film was reported. The position of the Al 2*p* peak at 75.43 (see Fig. 2) indicates the presence of Al<sup>3+</sup> state (corresponding to anhydrous oxide).<sup>6,21,22</sup> The absence of any other feature in the Al 2*p* spectra shows that no Al<sup>0</sup> is present. XPS analysis of the same samples obtained at 30° gives identical binding energies indicating homogeneous composition in the film. The FTIR and XPS analyses of *as-deposited* films show that neither any aluminum silicate phase nor any silicon oxide is present at the film–substrate interface.

O/Al ratio in aluminum oxide depends on the process conditions<sup>6,15</sup> and values as high as 1.85 had been previously reported.<sup>23</sup> The O/Al ratio in the deposited film was calculated using the integrated intensities of the Al 2*p* and O 1*s* peaks and atomic sensitivity factors for Al and O. The ratio was found to be  $\sim 2.1$ , which is 40% higher than that for stoichiometric  $\text{Al}_2\text{O}_3$ . The slightly higher value of the binding energy of the Al<sup>3+</sup> states can be explained by considering the presence of excess oxygen in the system.

Aluminum oxide films deposited at 300 °C were annealed in Ar at 900 °C. A FTIR spectrum of a sample annealed for 25 min is shown in Fig. 1(b). The strong absorption band at 1058  $\text{cm}^{-1}$  is identical to the TO mode arising from the asymmetric stretching of O in Si—O—Si, in thermally grown<sup>24,25</sup> amorphous silicon dioxide (*a*-SiO<sub>2</sub>). The intensity of this peak increased rapidly with annealing time before reaching a constant value. This indicates that on annealing an *as-deposited* sample, a SiO<sub>2</sub> layer is formed between the deposited alumina film and the Si(100) substrate.

Figure 3(a) shows a high-resolution Z-contrast image of a 5 nm deposited film annealed for 25 min in Ar at 900 °C. The Si substrate is located at the bottom of the micrograph and the individual atomic Si columns in the (110) direction

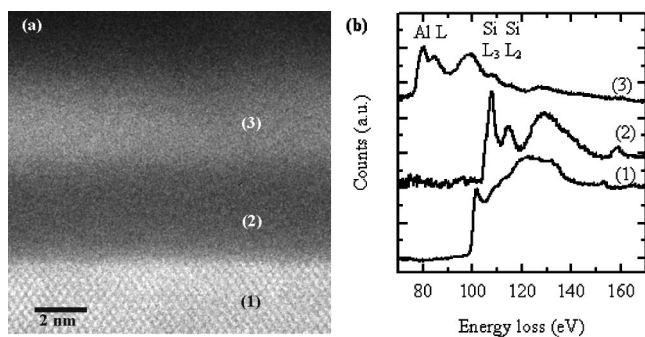


FIG. 3. Aluminum-oxide film, annealed at 900 °C in Ar for 25 min. (a) Z-contrast image (spatial resolution  $\sim 2$  Å) with location of EELS analysis indicated. (b) Background subtracted and multiple scattering corrected EELS spectra (acquisition time 0.5 s; energy resolution 1.0 eV) showing Si and Al edges.

are visible. The dark region (5 nm) in between the Si and the brighter  $\text{Al}_2\text{O}_3$  film indicates the  $\alpha$ - $\text{SiO}_2$ . Figure 3(b) displays EELS spectra taken from the position indicated in Fig. 3(a). The spectrum from the Si substrate contains an edge onset at  $(99.8 \pm 0.5)$  eV due to  $\text{Si}^0$  contribution<sup>26</sup> but no distinct white line intensities that would indicate a native oxide. The silicon-oxide layer shows a shift of the edge onset of  $(6.2 \pm 0.5)$  eV and a distinct  $L_3$ ,  $L_2$  splitting. This can be interpreted as being caused by a change from predominantly  $\text{Si}^0$  to predominantly  $\text{Si}^{4+}$  contributions to the spectrum. No aluminum signal is detected, thus indicating a pure  $\text{SiO}_2$  layer. The deposited film spectrum contains a strong Al peak characteristic<sup>27,28</sup> of  $\text{Al}_2\text{O}_3$  and no measurable intensities at either the  $\text{Si}^0$  or the  $\text{Si}^{4+}$  core-loss onsets. The presence of the oxide layer can be explained by considering diffusion of the excess oxygen present in the film (as seen in the XPS analysis) toward the Si substrate and reaction to form  $\text{SiO}_2$  upon annealing.

In this study, we addressed the interfacial chemistry of aluminum-oxide films deposited on Si(100). A combination of FTIR, XPS, STEM, and EELS analyses was used to probe *as-deposited* films and the effect of annealing in an inert environment. The findings of this study are:

- (i) Low-temperature MOCVD of aluminum-oxide films on Si using TMA and  $\text{O}_2$  does not give rise to any aluminum-silicate layer. No detectable  $\text{SiO}_2$  layer is formed during such a deposition process.
- (ii) The deposition carried out using  $\text{O}_2$  and TMA may result in an O/Al ratio higher than that in stoichiometric  $\text{Al}_2\text{O}_3$ ; and
- (iii) Postdeposition annealing of the films at 900 °C gives rise to an  $\alpha$ - $\text{SiO}_2$  layer at the film–substrate interface.

Diffusion of excess oxygen in the deposited aluminum-oxide film is apparently responsible for the formation of the interfacial  $\text{SiO}_2$  layer.

Experimental results were obtained on the JEOL 2010F, operated by the Research Resources Center at UIC and funded by the NSF under Grant No. DMR-9601796. This research was supported in part by the NSF under Grant Nos. DMR-9733895 and CTS 9813984. The XPS data were obtained at the Center for Microanalysis of Materials, UIUC supported by the U.S. Department of Energy under Grant No. DEFG02-96-ER45439.

- <sup>1</sup>G. D. Wilk, R. M. Wallace, and J. M. Anthony, *J. Appl. Phys.* **89**, 5243 (2001).
- <sup>2</sup>S. Guha, E. Cartier, N. A. Bojarczuk, J. Bruley, L. Gignac, and J. Karasinski, *J. Appl. Phys.* **90**, 512 (2001).
- <sup>3</sup>V. A. C. Haanappel, H. D. van Corbach, T. Franssen, and P. J. Gellings, *Surf. Coat. Technol.* **72**, 13 (1995).
- <sup>4</sup>E. P. Gusev, M. Copel, and E. Cartier, *Appl. Phys. Lett.* **76**, 176 (2000).
- <sup>5</sup>T. M. Klein, D. Niu, W. S. Epling, W. Li, D. M. Maher, C. C. Hobbs, R. I. Hegde, I. J. R. Baumvol, and G. N. Parsons, *Appl. Phys. Lett.* **75**, 4001 (1999).
- <sup>6</sup>Y.-C. Kim, H.-H. Park, J. S. Chun, and W.-J. Lee, *Thin Solid Films* **237**, 57 (1994).
- <sup>7</sup>B. S. Ault, *J. Organomet. Chem.* **572**, 169 (1999).
- <sup>8</sup>Z. Cui, J. Madsen, and C. G. Takoudis, *J. Appl. Phys.* **87**, 8181 (2000).
- <sup>9</sup>E. M. James and N. D. Browning, *Ultramicroscopy* **78**, 125 (1999).
- <sup>10</sup>E. M. James, N. D. Browning, A. W. Nicholls, M. Kawasaki, Y. Xin, and S. Stemmer, *J. Electron Microsc. J.* **47**, 561 (1998).
- <sup>11</sup>R. F. Egerton, *Electron Energy-Loss Spectroscopy in the Electron Microscope* (Plenum, New York, 1986).
- <sup>12</sup>N. D. Browning, M. F. Chrisholm, and S. J. Pennycook, *Nature (London)* **366**, 143 (1993).
- <sup>13</sup>P. D. Nellist and S. J. Pennycook, *Ultramicroscopy* **78**, 111 (1999).
- <sup>14</sup>D. E. Jesson and S. J. Pennycook, *Proc. R. Soc. London, Ser. A* **449**, 273 (1995).
- <sup>15</sup>Z. Katz-Tsameret and A. Raveh, *J. Vac. Sci. Technol. A* **13**, 1121 (1995).
- <sup>16</sup>R. Cuff, G. Baud, M. Benmalek, J. P. Besse, J. R. Butruille, H. M. Dunlop, and M. Jacquet, *Thin Solid Films* **270**, 230 (1995).
- <sup>17</sup>P. Tarte, *Spectrochim. Acta, Part A* **23**, 2127 (1967).
- <sup>18</sup>C. Morterra and G. Magnacca, *Catal. Today* **27**, 497 (1996).
- <sup>19</sup>M. P. Kumar, C. Balasubramanian, N. D. Sali, S. V. Bhoraskar, V. K. Rohatgi, and S. Badrinarayanan, *Mater. Sci. Eng., B* **63**, 215 (1999).
- <sup>20</sup>W. R. Salenek, R. Bergman, J.-E. Sundgren, A. Rockett, T. Motooka, and J. E. Green, *Surf. Sci.* **198**, 461 (1988).
- <sup>21</sup>Q. Wang, W. Zhao, J. Lozano, Y.-M. Sun, C. G. Willson, and J. M. White, *Appl. Surf. Sci.* **183**, 182 (2001).
- <sup>22</sup>E. Paparazzo, *Vacuum* **62**, 47 (2001).
- <sup>23</sup>B. G. Segda, M. Jacquet, and J. P. Besse, *Vacuum* **62**, 27 (2001).
- <sup>24</sup>A. Pasquarello and R. Car, *Phys. Rev. Lett.* **79**, 1766 (1997).
- <sup>25</sup>K. T. Queeney, M. K. Weldon, J. P. Chang, Y. J. Chabal, A. B. Gurevich, J. Sapjeta, and R. L. Opila, *J. Appl. Phys.* **87**, 1322 (2000).
- <sup>26</sup>P. E. Batson, *Nature (London)* **366**, 727 (1993).
- <sup>27</sup>M. Halvarsson, A. Larsson, and S. Ruppi, *Micron* **32**, 807 (2001).
- <sup>28</sup>K. Suenaga, D. Bouchet, C. Colliex, A. Thorel, and D. G. Brandon, *J. Eur. Ceram. Soc.* **18**, 1453 (1998).